



# Reconciling theories of dominance with the relative rates of adaptive substitution on sex chromosomes and autosomes

Yasmine McDonough<sup>a</sup> , Filip Ruzicka<sup>ab</sup> , and Tim Connallon<sup>a,1</sup>

Edited by Marcus Feldman, Stanford University, Stanford, CA; received March 27, 2024; accepted September 16, 2024

The dominance of beneficial mutations is a key evolutionary parameter affecting the rate and genetic basis of adaptation, yet it is notoriously difficult to estimate. A leading method to infer it is to compare the relative rates of adaptive substitution for X-linked and autosomal genes, which—according to a classic model by Charlesworth et al. (1987)—is a simple function of the dominance of new beneficial mutations. Recent evidence that rates of adaptive substitution are faster for X-linked genes implies, accordingly, that beneficial mutations are usually recessive. However, this conclusion is incompatible with leading theories of dominance, which predict that beneficial mutations tend to be dominant or overdominant with respect to fitness. To address this incompatibility, we use Fisher's geometric model to predict the distribution of fitness effects of new mutations and the relative rates of positively selected substitution on the X and autosomes. Previous predictions of faster-X theory emerge as a special case of our model in which the phenotypic effects of mutations are small relative to the distance to the phenotypic optimum. But as mutational effects become large relative to the optimum, we observe an elevated tempo of positively selected substitutions on the X relative to the autosomes across a broader range of dominance conditions, including those predicted by theories of dominance. Our results imply that, contrary to previous models, dominant and overdominant beneficial mutations can plausibly generate patterns of faster-X adaptation. We discuss resulting implications for genomic studies of adaptation and inferences of dominance.

adaptation | dominance | sex chromosomes | mutation | population genetics

Genetic dominance plays a pivotal role in evolution. Indeed, a comprehensive understanding of dominance is required to explain a wide array of evolutionary phenomena (1), including the evolution of sex, the genetic basis of adaptation, and the maintenance of genetic variation in life history traits (2–5). Dominance is also a key determinant of population viability, as it affects genetic load and inbreeding depression (6, 7), rates of adaptation (8–10), and probabilities of extinction following environmental change (11).

Despite its importance, data on the distribution of dominance for beneficial mutations remain severely limited (1, 9). Mutation accumulation and gene knockout experiments provide compelling evidence that deleterious mutations are, on average, partially recessive with respect to fitness (12–15), yet the rarity of spontaneous beneficial mutations (relative to deleterious ones) hinders systematic estimates of their fitness effects (9, 16). Most information about beneficial mutations is based on case studies of the genetics of adaptation, which report a range of dominance effects (e.g., refs. 17–20), including overdominance [i.e., heterozygote advantage; (21, 22)]. However, there are many reasons why such variants might not be representative of new beneficial mutations, including biases in the relative rates of establishment for dominant versus recessive mutations [i.e., “Haldane's sieve” (8, 23)].

Given the difficulty of directly estimating the dominance of beneficial mutations, an indirect inference approach—based on empirical comparisons between the adaptive substitution rates of sex chromosomes and autosomes—has grown in popularity and feasibility over the last two decades. The approach draws from an influential theory paper by Charlesworth et al. (24), which modeled the substitution rates of positively selected mutations on the X chromosome and autosomes. Using a simple population genetic model, Charlesworth et al. (24) showed that the substitution rate is faster for X-linked genes if beneficial mutations are partially or completely recessive with respect to fitness ( $0 \leq h < 0.5$ ), whereas autosomal genes adapt faster when beneficial mutations are dominant ( $0.5 < h \leq 1$ ; see Fig. 1A). This theory has since been extended to include adaptation from standing genetic variation (23, 25, 26), X-linked genes with functional Y-linked homologs (27), and species- and sex-specific variability in population sizes and mutation rates (28–30). Overall, these models imply that faster-X patterns are unlikely to emerge unless beneficial mutations often have recessive fitness effects.

## Significance

The fitness effects of beneficial mutations, including their degrees of dominance, are fundamental evolutionary quantities that are challenging to estimate. The theory of “faster-X” evolution posits that dominance with respect to fitness can be inferred by comparing rates of adaptation on the X chromosome and autosomes, with faster-X adaptation indicating that beneficial mutations are recessive. In view of this theory, the mounting evidence for faster-X adaptation implies that beneficial mutations are often recessive, yet this interpretation contradicts leading explanations for dominance itself, which predict that beneficial mutations should more often be dominant than recessive. Our model shows that conditions for faster-X adaptation are broader than previously thought and compatible with leading explanations for dominance.

Author affiliations: <sup>a</sup>School of Biological Sciences, Monash University, Clayton, VIC 3800, Australia; and <sup>b</sup>Institute of Science and Technology Austria, Klosterneuburg 3400, Austria

Author contributions: Y.M., F.R., and T.C. designed research; Y.M. and T.C. performed research; F.R. analyzed data; Y.M., F.R., and T.C. edited versions of the paper; and Y.M. and T.C. wrote the paper.

The authors declare no competing interest.

This article is a PNAS Direct Submission.

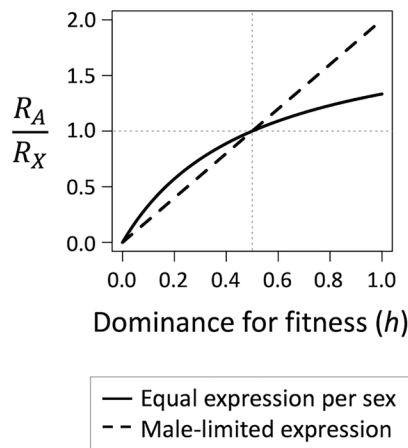
Copyright © 2024 the Author(s). Published by PNAS. This article is distributed under [Creative Commons Attribution-NonCommercial-NoDerivatives License 4.0 \(CC BY-NC-ND\)](https://creativecommons.org/licenses/by-nc-nd/4.0/).

<sup>1</sup>To whom correspondence may be addressed. Email: [tim.connallon@monash.edu](mailto:tim.connallon@monash.edu).

This article contains supporting information online at <https://www.pnas.org/lookup/suppl/doi:10.1073/pnas.2406335121/-/DCSupplemental>.

Published October 22, 2024.

### A Classical faster-X theory



### B Adaptive substitution rate estimates

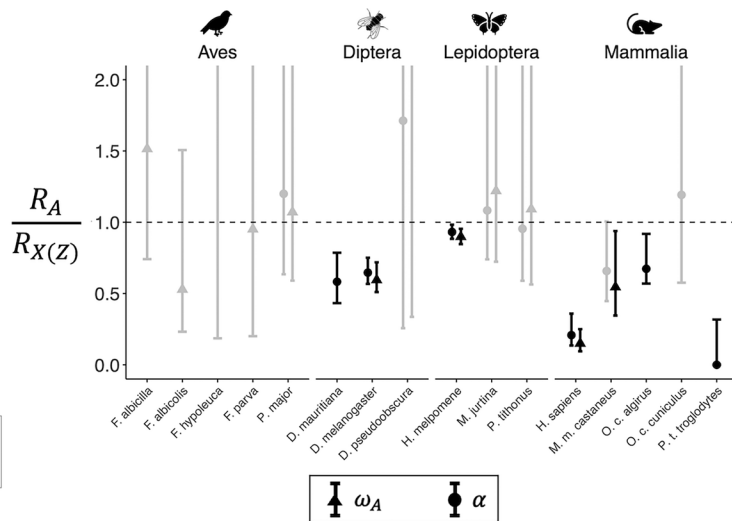


**Fig. 1.** Classical faster-X theory and current estimates of adaptive substitution rates on sex chromosomes (the X or Z) and autosomes. (A) The relative rates of selective sweeps for autosomal ( $R_A$ ) relative to sex-linked genes ( $R_X$ ) predicted by Charlesworth et al. (24), under the assumptions outlined in the beginning of the Results section. A faster-X pattern ( $R_A/R_X < 1$ ) is expected when beneficial mutations are partially-to-completely recessive ( $h < 0.5$ ). (B) Estimates ( $\pm 95\%$  CIs) of the adaptive substitution rate [ $\omega_A$ , which is standardized by the neutral substitution rate (31)] and the proportion of substitutions fixed by positive selection ( $\alpha$ ) for autosomal versus sex-linked genes. 95% CIs were calculated as Lower95 $_X$ /Upper95 $_X$  and Upper95 $_X$ /Lower95 $_X$ , with significant deviations (where the 95% CIs do not overlap 1) shown in black. Estimates are based on 11 studies—out of a total of 16 (Supplementary Dataset)—in which CI were reported and corrections were made for segregating nonneutral polymorphisms (32–42).

The adaptive substitution rates of sex chromosomes and autosomes have now been estimated in several species (summarized in Fig. 1B), with many studies reporting strongly elevated rates of X-linked substitution (e.g., refs. 26, 32–37, 43), and none finding significant faster-autosome patterns. *Drosophila* genomes also show enriched signals of recent, “hard” selective sweeps on the X relative to the autosomes (44, 45). These observations, when interpreted under faster-X theory, suggest that beneficial mutations tend to have recessive fitness effects. For example, Charlesworth et al. (26) surveyed a range of possible causes underlying the *Drosophila* data, and concluded that they were consistent with beneficial mutations having partially recessive fitness effects on average (i.e., the *Drosophila* estimates, in the range  $R_A/R_X \approx 0.5 - 0.67$ , implied a mean dominance of  $h \approx 0.17 - 0.25$ ).

The combination of faster-X theory and evidence for adaptive faster-X evolution in several animal lineages implies that beneficial mutations might typically be recessive, yet leading theories of dominance predict the opposite. In physiological theories of dominance, a diminishing-return relationship between enzyme activity and rates of flux through metabolic pathways causes deleterious mutations (i.e., those with reduced enzyme activity) to be partially recessive (46–48) and beneficial mutations that increase activity to be dominant (49). Another strand of theory, based on Fisher’s geometric model, considers the fitness effects of mutations affecting traits selected to an optimum (Fig. 2). The nonlinear relation between trait expression and fitness in the vicinity of the optimum causes deleterious mutations to be partially recessive and beneficial mutations to be partially dominant or overdominant (Fig. 2; see refs. 14, 50). Both models are consistent with observations about the dominance of deleterious mutations (for which we have direct, reliable, and unbiased estimates) and they predict that beneficial mutations should often exhibit relatively dominant fitness effects.

Dominance inferred from faster-X theory and data on the one hand (Fig. 1), and dominance predicted from models of enzyme activity or Fisher’s geometric model on the other (Fig. 2), therefore generate conflicting conclusions. How can we resolve this conflict?

A potential clue to a resolution lies in a key assumption in previous models of faster-X adaptation: that adaptive mutations have intermediate heterozygous fitness effects (i.e.,  $0 < h < 1$ ) and, thus, are never overdominant. In contrast, Fisher’s geometric model (14, 50) and supporting experimental work (21, 22) suggest that a substantial fraction of adaptive mutations might be overdominant with respect to fitness (Fig. 2B). Crucially, the evolutionary dynamics of overdominant mutations differ between the X and autosomes, with overdominance expected to maintain polymorphism on autosomes, whereas the haploid expression of X-linked genes in males can lead

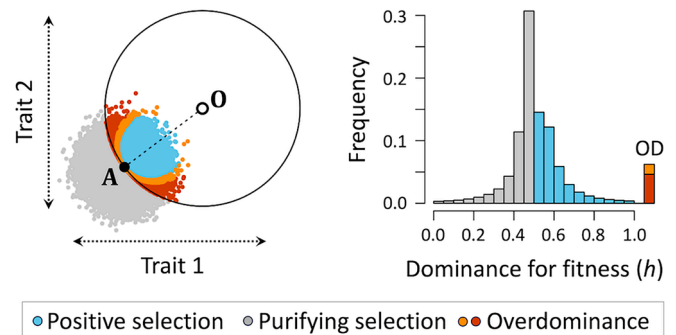


**Fig. 2.** Selection and dominance in Fisher’s geometric model with two traits. The example on the left shows an ancestral genotype (with phenotype A) that is displaced from the optimum (phenotype O). The phenotypes of individuals heterozygous for random mutations are scattered around the ancestral type, and fitness declines as a Gaussian function of the distance to the optimum. Following Manna et al. (14), this example assumes that there is no dominance between alleles with respect to their effects on trait expression. However, the nonlinear (Gaussian) relation between phenotype and fitness generates dominance with respect to fitness. Mutant fitness effects are categorized by color, with blue and gray dots representing mutations subject to positive and purifying selection in diploids, respectively. The red and orange dots are subject to balancing selection in diploids. A subset of overdominant mutations (orange ones in this example) will experience positive selection when X-linked, along with the blue mutations that are positively selected on both chromosome types. The distribution of dominance with respect to fitness (the parameter  $h$ ) is shown on the right, with adaptive variants exhibiting partial dominance ( $0.5 < h < 1$ ; blue) or overdominance (orange and red); deleterious variants are partially recessive ( $0 < h < 0.5$ ).

to rapid fixation of overdominant alleles on the X (51, 52). Overdominant mutations might, therefore, contribute substantially to positively selected substitutions on the X but not the autosomes, resulting in an overall faster tempo of X-linked adaptive substitutions without the need to invoke recessive fitness effects of beneficial mutations.

Here, we use Fisher's geometric model (14, 50, 53–57) to generate predictions about the relative rates of positively selected substitutions on X chromosomes and autosomes. Following previous models of faster-X adaptation, we focus on evolutionary scenarios in which adaptation uses new beneficial mutations. This assumption allows us to directly link our results to prior faster-X models while retaining analytical tractability (we provide a broader discussion of this assumption and its consequences in the Discussion). In contrast to previous models of faster-X adaptation, where the fitness effects of beneficial mutations are simply assumed, we explicitly model the distribution of fitness effects for new beneficial mutations, which in Fisher's geometric model emerges naturally from a biologically plausible scenario in which traits are selected to an optimum (Fig. 2). From this distribution, we predict rates of positively selected substitutions on each chromosome type and reexamine their sensitivities to dominance.

## Results

**Baselines Under Classical Faster-X Theory.** We begin by outlining the modeling framework of Charlesworth et al. (24), upon which prior predictions of faster-X adaptive evolution are based (for elaborations, see refs. 25–30). Assuming an XY sex chromosome system, an equal sex ratio among breeding adults, and equivalent phenotypic and fitness effects of mutations when expressed in homo- versus hemizygous state, Charlesworth et al. (24) showed that the rate of positively selected substitutions on autosomes versus the X chromosome is a function with two parts: (i) the relative rates of mutation to positively selected alleles on each chromosome ( $\mu_A$  and  $\mu_X$  per autosomal and X-linked gene, respectively), and (ii) the relative probabilities of fixation for positively selected alleles on each chromosome ( $\Pi_A$  and  $\Pi_X$ ). The rate of substitution for the autosomes ( $R_A$ ) relative to the X ( $R_X$ ) can then be expressed as:

$$\frac{R_A}{R_X} = \frac{4}{3} \cdot \frac{\mu_A}{\mu_X} \cdot \frac{\Pi_A}{\Pi_X} \quad [1]$$

By assuming that mutation rates to positively selected alleles are equal between X-linked and autosomal genes ( $\mu_A/\mu_X = 1$ ), and that each mutation's dominance with respect to fitness ( $h$ ) is in the range  $0 \leq h \leq 1$ , Charlesworth et al. (24) found that the ratio of fixation probabilities ( $\Pi_A/\Pi_X$ ) is a simple function of the dominance coefficients of positively selected mutations. For mutations with equal expression in each sex, the ratio of fixation probabilities is  $\Pi_A/\Pi_X = 3h/(1+2h)$ , making the relative rate of positively selected substitutions:

$$\frac{R_A}{R_X} = \frac{4h}{1+2h}, \quad [2]$$

(the solid curve in Fig. 1A). For mutations with male-limited expression, the ratios are  $\Pi_A/\Pi_X = 3h/2$  and:

$$\frac{R_A}{R_X} = 2h, \quad [3]$$

(the dashed curve in Fig. 1A). Eqs. 2 and 3 suggest that faster-X rates of adaptation require positively selected mutations to be partially or completely recessive with respect to fitness ( $0 \leq h < 0.5$ ).

Our model uses the same framework as depicted in Eq. 1, but our analysis differs from prior faster-X theory in that we explicitly model the relative rates of mutation to positively selected alleles, as well as their fitness effects and fixation probabilities (*Materials and Methods* for details). As in prior faster-X models, we focus on positively selected substitutions, which are expected to increase signals of adaptive substitution in population genomic data (58, 59). We later consider how mutations under balancing selection should affect signals of adaptive substitution on the X versus autosomes.

**Mutation Rates to Positively Selected Alleles.** Mutation rates to positively selected alleles depend on their phenotypic effect sizes, their degrees of dominance, and their modes of inheritance (i.e., autosome or X-linkage). Following previous versions of Fisher's model (53, 54), we define the scaled size of a mutation as  $x = r\sqrt{n}/(2z)$ , where  $r$  is the absolute phenotypic effect of the mutation in homozygotes,  $n$  is the number of traits, and  $z$  is the displacement of the population from the optimum. There are two measures of dominance in our model (14): dominance with respect to the phenotype ("phenotypic dominance" or  $v$ ) and dominance with respect to fitness ( $h$ ).

In the limit of infinitesimally small-scaled mutation sizes ( $x \rightarrow 0$ , where mutation sizes are small relative to the distance to the optimum), we observe that virtually all beneficial mutations are subject to positive selection (i.e., balancing selection is negligible) and dominance with respect to fitness is equivalent to dominance with respect to trait expression ( $h = v$ ; *SI Appendix, Appendix 3*). In this limit, mutation rates to positively selected alleles are equal between the X and autosomes ( $\lim_{x \rightarrow 0} \mu_A/\mu_X = 1$ ), as assumed by previous models of faster-X evolution.

As the scaled phenotypic effect size of a mutation increases, the probability that it experiences positive selection decreases. And because criteria for positive selection are more stringent on autosomes than the X, we observe a more rapid decrease for autosomal than X-linked genes (Fig. 3A). As the mean mutation size ( $\bar{x}$ ) becomes large, the distribution of mutation sizes across the interval of  $x$  where positive selection can occur ( $0 < x < 3$ , as illustrated in Fig. 3A) becomes uniform (see the Supplementary Text of ref. 50). In this "large-mutation limit", the autosome-to-X ratio of mutation rates to positively selected alleles becomes:

$$\frac{\mu_A}{\mu_X} = \frac{3 - 2v^2}{(3 - 2v)(1 + v)}. \quad [4]$$

Here, the mutation rate to positively selected alleles is greater on the X than the autosomes across the spectrum of phenotypic dominance ( $0 < v < 1$ ), with the discrepancy increasing with  $v$  (Fig. 3B). This is because mutations with high  $v$  include a substantial fraction of overdominant alleles that undergo positive selection when X-linked but not when autosomal. In the large-mutation limit, dominance with respect to fitness is larger than phenotypic dominance (the relation between  $\bar{h}$  and  $v$  is very roughly  $\bar{h} \approx v + v(1 - v)/(1 + 2v)$ ; *SI Appendix, Appendix 3*), but a similar bias toward the X is observed when plotting  $\mu_A/\mu_X$  against mean dominance for fitness ( $\bar{h}$ ) among mutations that are positively selected on both chromosome types (i.e.,  $s_{hom} \geq s_{het} \gg 0$ , where  $s_{het}$  and  $s_{hom}$  denote heterozygous and homozygous fitness effects).

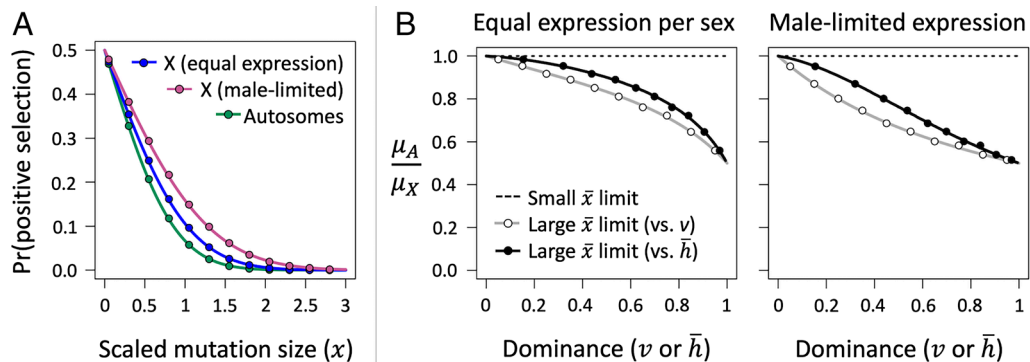


**Fig. 3.** Mutation rates to positively selected alleles at autosomal and X-linked genes. (A) Probability that a random mutation, with scaled mutation size of  $x$  and phenotypic dominance of  $v = 0.5$ , meets conditions for positive selection. Curves are based on Eqs. 13a and 13b, and each circle is based on  $10^5$  simulated mutations. (B) Ratios of mutation rates to positively selected alleles at autosomal and X-linked genes, plotted as a function of phenotypic dominance ( $v$ ) or mean dominance with respect to fitness (values of  $\bar{h}$  are each a function of  $v$ ). Dashed curves represent predictions for the small-mutation limit (i.e.,  $\mu_A/\mu_X = 1$ ). Solid curves are solutions for the large-mutation limit (Eqs. 4 and 5) and circles are based on  $10^5$  simulated mutations. Simulations assume that  $z = 1$  and  $n = 50$ ; in panel B, values of  $x$  are drawn from a uniform distribution ( $0 < x < 10$ ).

Under male-limited expression, the small-mutation limit again converges to  $\lim_{x \rightarrow 0} \mu_A/\mu_X = 1$ , while the large-mutation limit becomes:

$$\frac{\mu_A}{\mu_X} = \frac{1}{1+v}, \quad [5]$$

which again yields an elevated mutation rate to positively selected alleles on the X relative to the autosomes (Fig. 3B).

**Fixation Probabilities of Positively Selected Mutations.** For a new mutation to become fixed, it must escape stochastic loss when it is rare. We therefore calculate the fixation probability of mutations that meet conditions for positive selection. In the small-mutation limit, the probability that a random, positively selected mutation becomes fixed on the autosomes relative to the X matches the classic prediction from Charlesworth et al. (24) ( $\lim_{x \rightarrow 0} \Pi_A/\Pi_X = 3v/(2v+1) = 3h/(2h+1)$ ). Here, fixation probabilities are consistently higher on the X (Fig. 4) because haploid expression of X-linked genes in males increases the strength of selection for rare, positively selected variants (52).

In the large-mutation limit, the ratio of fixation probabilities becomes:

$$\frac{\Pi_A}{\Pi_X} = \frac{3v(3+v)(3-2v^2)^2}{(1+v)^2(3-2v)(3+2v(1-v)(2v+1))}, \quad [6]$$

which aligns well with simulated data (Fig. 4) and predicts an even stronger X-linked bias for the fixation probability of positively selected mutations (Fig. 4). The stronger bias reflects a somewhat higher average fitness effect of positively selected alleles on the X relative to autosomes.

For male-limited genes, the small-mutation limit once again matches the result from Charlesworth et al. (24) ( $\lim_{x \rightarrow 0} \Pi_A/\Pi_X = 3v/2 = 3h/2$ ). In the large-mutation limit, this ratio becomes:

$$\frac{\Pi_A}{\Pi_X} = \frac{3v(3+v)}{2(1+v)^2}, \quad [7]$$

which shows a weaker bias toward the X than previous results (Fig. 4). The change reflects an abundance of weakly selected mutations

within the pool of positively selected X-linked variants, many of which would not evolve under positive selection on autosomes.

**Substitution Rates of Positively Selected Mutations.** The substitution rate for each chromosome is a function of the mutation rate to positively selected alleles and their fixation probabilities. In the small-mutation limit, and assuming equal gene expression in each sex, the substitution rate for autosomal relative to X-linked genes simplifies to the classic prediction of Charlesworth et al. (24) ( $\lim_{x \rightarrow 0} R_A/R_X = 4v/(1+2v) = 4h/(1+2h)$ ). Consequently, the rate is higher for the X than the autosomes when mutations tend to be recessive ( $v = h < 0.5$  for  $x \rightarrow 0$ ) and slower on the X when mutations are dominant ( $v = h \gg 0.5$ ).

In the large-mutation limit, the ratio becomes:

$$\frac{R_A}{R_X} = \frac{4v(3+v)(3-2v^2)^3}{(1+v)^3(3-2v)^2(3-2v(v-1)(2v+1))}, \quad [8]$$

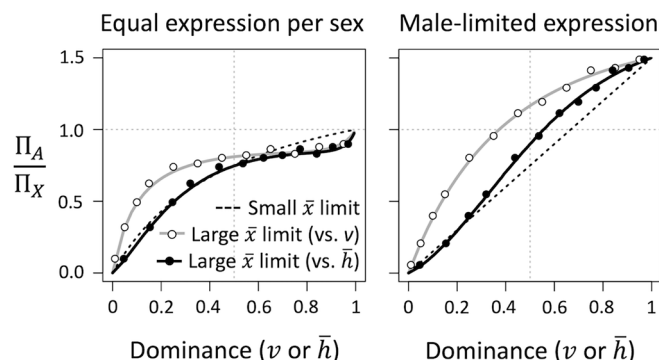


**Fig. 4.** Fixation probabilities of positively selected mutations on the autosomes and X. The dashed curves represent predictions for the small-mutation limit (i.e.,  $\Pi_A/\Pi_X = 3v/(2v+1)$  for equal expression and  $\Pi_A/\Pi_X = 2v$  for male-limited expression). The solid curves are solutions for the large-mutation limit (Eqs. 6 and 7), plotted as a function of phenotypic dominance ( $v$ ) and dominance with respect to fitness ( $\bar{h}$ , in black). Circles are based on Wright-Fisher simulations (5,000 replicates each) of the proportion of random, positively selected mutations on each chromosome that are eventually fixed. Simulations assume that  $z = 1$  and  $n = 50$ , with scaled mutation sizes ( $x$ ) for new mutations drawn from a uniform distribution ( $0 < x < 10$ ), and Wright-Fisher simulations carried out for the subset that met criteria for positive selection on each chromosome type.

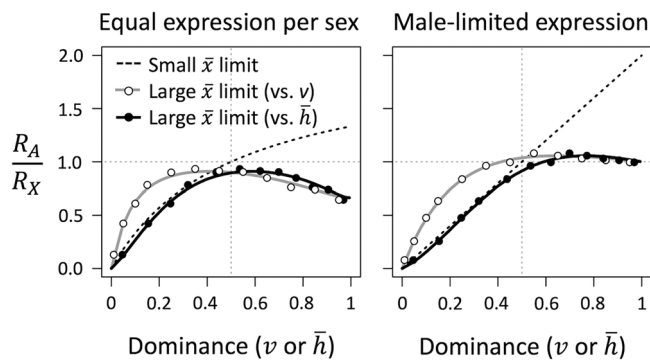


**Fig. 5.** Relative rates of positively selected substitutions on the autosomes relative to the X chromosome. The dashed curves apply to the small-mutation limit (Eqs. 2 and 3). Solid curves apply to the large-mutation limit (Eqs. 8 and 9), plotted as a function of phenotypic dominance ( $v$ , in gray) and dominance with respect to fitness ( $\bar{h}$ , in black). Circles are based on Wright–Fisher simulations, 5,000 fixation events each. Simulations assume that  $z = 1$  and  $n = 50$ , with scaled mutation sizes ( $x$ ) for new mutations drawn from a uniform distribution ( $0 < x < 10$ ), and Wright–Fisher simulations carried out for the subset that meets criteria for positive selection.

which results in a consistently higher X-linked substitution rate across the spectrum of dominance (Fig. 5). This consistent bias toward the X arises because recessive mutations are much more efficiently selected on the X (Fig. 4), while dominant mutations are much more likely to meet criteria for positive selection on the X (Fig. 3B). Indeed, if we assume that phenotypic dominance for random mutations follows a standard uniform distribution (i.e., uniform within the range:  $0 < v < 1$ ), then  $R_A/R_X \approx 0.79$ , corresponding to a 27% higher rate of substitution on the X. If all mutations have codominant phenotypic effects ( $v = 0.5$ ), the rate is 11% higher on the X.

For male-limited genes in the small-mutation limit, we again retrieve the classic result ( $\lim_{x \rightarrow 0} R_A/R_X = 2v = 2h$ ; see Eq. 4 of ref. 24). In the large-mutation limit, we obtain:

$$\frac{R_A}{R_X} = \frac{2v(3+v)}{(1+v)^3} \quad [9]$$

where male-limited genes exhibit more rapid substitution rates on the X when mutations are recessive, and the substitution rates are roughly equal between chromosomes when mutations are codominant-to-dominant (Fig. 5). Under a uniform distribution of phenotypic dominance ( $0 < v < 1$ ), the ratio of substitution rates becomes  $R_A/R_X \approx 0.89$  (~12% higher for the X). Under a purely codominant model ( $v = 0.5$ ), Eq. 9 simplifies to  $R_A/R_X \approx 1.04$ .

**Substitution Rates Due to Positively Selected and Balanced Polymorphisms.** We have focused on the substitution rates of positively selected mutations, which are expected to fix rapidly and thereby contribute to empirical signals of adaptive substitution (e.g., long-term signals derived from McDonald–Kreitman or “MK” tests, or comparatively recent signals of hard selective sweeps; see refs. 45, 58, 60). But our analytical predictions do not yet account for balanced polymorphisms, whose fixation rates can sometimes be faster than those of neutral variants (61, 62). Moreover, fixation of mutations under balancing selection might be more common on autosomes than the X because autosomes are a more permissive environment for overdominant balancing selection.

To evaluate this possibility, we carried out simulations that tracked the evolutionary dynamics of mutations with deterministic equilibrium frequencies above 50% [mutations with equilibria

below this threshold are unlikely to fix (62)] and recorded the number of autosomal and X-linked substitutions that fixed more rapidly than the standard neutral benchmarks of  $4N$  generations for the autosomes and  $3N$  generations for the X (52, 63). We find that our analytical predictions hold up well across most conditions of dominance (Fig. 6). Indeed, it is only as phenotypic dominance approaches one ( $v \rightarrow 1$ ) that balanced polymorphic substitutions noticeably shift the simulated values of  $R_A/R_X$  away from our analytical results based on positively selected substitutions alone. The deviation between simulated and analytical results is more pronounced in small than large populations (Fig. 6), which likely reflects the stronger efficacy of balancing selection—and thus, the longer segregation times of balanced polymorphisms—in large populations (for related results, see ref. 64).

**Substitution Rates in Populations Segregating for Balanced Polymorphisms.** The results presented above focus on substitutions in initially monomorphic populations. To test how these substitution rates might be affected by balanced polymorphisms initially segregating at other loci, we developed two extensions of our model: one with new mutations completely linked to a balanced polymorphic locus (*SI Appendix, Appendix 3 and SI Appendix, Fig. S3*) and one with mutations unlinked to the polymorphic locus (*SI Appendix, Appendix 5 and SI Appendix, Fig. S4*). In both cases, we assumed that a balanced polymorphism initially segregates at an intermediate frequency on either the X or an autosome. Homozygotes for the polymorphic locus initially express phenotypes that are equally distant from the optimum (these phenotypes are labeled  $A_{11}$  and  $A_{22}$  in Fig. 7A). The strength of overdominance, which maintains the polymorphism, is a function of the phenotypic distance between these homozygotes (denoted  $r$  in Fig. 7A) and the angle between the displacements of each homozygote from the optimum ( $\theta$  in Fig. 7A). For simplicity, we assume that segregating and new mutations have

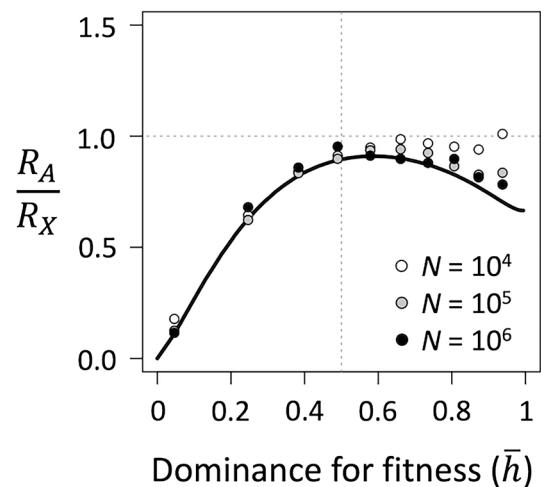


**Fig. 6.** Rates of adaptive substitution on the autosomes and X, including both balanced and positively selected mutations that fixed more rapidly than the average neutral substitution. Analytical results (the curve) show the ratio of positively selected substitution rates (Eq. 8: the large-mutation limit with genes expressed by both sexes). Circles show simulations of the relative numbers of substitutions fixed on the autosomes and X for three population sizes:  $N = 10^4$ ,  $N = 10^5$ , and  $N = 10^6$ . Results are based on Wright–Fisher simulations with  $z = 1$ ,  $n = 50$ , and scaled mutation sizes ( $x$ ) for new mutations drawn from a uniform distribution ( $0 < x < 3$ , with the limits chosen for computational efficiency). Simulations were carried out for mutations with deterministic equilibria above 0.5. Autosomal substitutions recorded fixation events that occurred prior to generation  $4N$ , and X-linked substitutions recorded fixations that preceded generation  $3N$ . Each simulated datapoint is based on 10,000 fixation events (for population sizes  $N = 10^4$  and  $N = 10^5$ ) or 1,000 fixation events (for population size  $N = 10^6$ ).

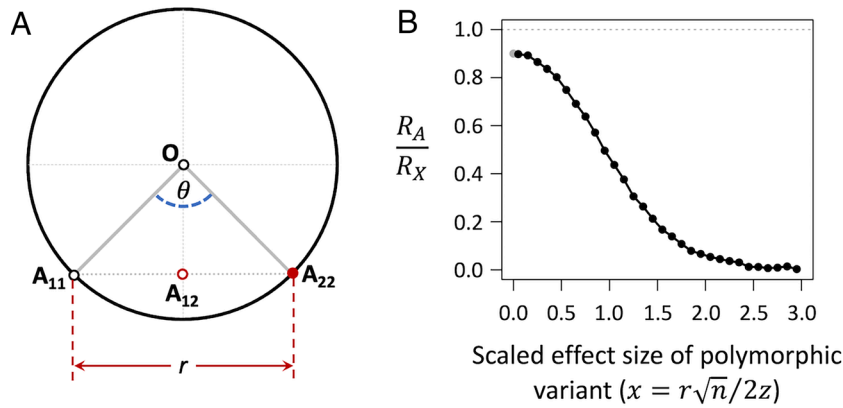


**Fig. 7.** Rates of adaptive substitution in populations initially segregating for a balanced polymorphism. (A) Visualization of the geometry of an intermediate-frequency balanced polymorphism maintained by heterozygote advantage. Homozygotes for the ancestral polymorphism express phenotypes  $A_{11}$  and  $A_{22}$ , which are equidistant from the optimum ( $z$  is the distance of each from  $O$ ).  $\theta$  represents the angle between the homozygote orientations of displacement from the optimum, which places the heterozygote phenotype closer ( $z_{12} = z\sqrt{1 - (r/(2z))^2}$  is the distance of the heterozygote from the optimum). (B) Relative rates of positively selected substitutions of mutations arising in tight linkage with a balanced polymorphism of scaled effect size  $x$ . Simulated results (black circles, each based on  $10^7$  fixations events per chromosome) are based on the model described in *SI Appendix, Appendix 4*. The gray point shows the analytical approximation for positively selected substitutions occurring in initially monomorphic populations, which is equivalent to the prediction for substitutions of mutations that are unlinked to the balanced polymorphism (*SI Appendix, Appendix 5*). Simulations assume that  $z = 1$  and  $n = 50$ , with scaled mutation sizes for new mutations drawn from a uniform distribution ( $0 < x < 3$ ) (i.e., in the “large-mutation limit”), and Bernoulli sampling used to simulate fixation or loss of mutations that meet criteria for positive selection (*SI Appendix, Appendix 4*).

codominant effects within and between loci (i.e., phenotypic dominance is  $v = 0.5$ ).

Complete linkage to a balanced polymorphism (*SI Appendix, Appendix 4*) decreases the potential for a new mutation to spread in the population, and this dampening effect is larger for loci linked to an autosomal polymorphism compared to loci linked to an X-linked polymorphism (Fig. 7B). Specifically, as the phenotypic distance between homozygotes of the balanced polymorphism increases (i.e., expressed as the scaled distance,  $x = r\sqrt{n}/(2z)$ , in Fig. 7B), positively selected substitution rates become increasingly biased toward the X relative to the autosomes. Consequently, our results for initially monomorphic populations are conservative and, if anything, underestimate the extent to which positively selected substitutions are elevated on the X relative to the autosomes.

A balanced polymorphism also reduces the potential for positive selection at unlinked loci (*SI Appendix, Appendix 5*) by elevating the effective pleiotropy of mutations that arise at other locations in the genome (i.e., their effective dimensionality; see refs. 65, 66). Specifically, a balanced polymorphism elevates effective dimensionality by a factor of  $2/(1 + \cos(\theta))$  (e.g., dimensionality effectively doubles when homozygotes for the polymorphic locus have orthogonal displacements from the optimum), which dampens the potential for positive selection and the probability of fixation at unlinked loci. This dampening effect is, however, the same for the X and autosomes, resulting in no net change to their *relative* adaptive substitution rates when compared to a monomorphic population.

## Discussion

Predictions of traditional faster-X models [(24, 26); Fig. 1A] rest on two critical assumptions: 1) that adaptation proceeds by the fixation of new, positively selected mutations, as opposed to beneficial alleles drawn from standing genetic variation; and 2) that the proportion of mutations that experience positive selection and the selection coefficients associated with positively selected alleles are equivalent between the X and autosomes. Models that relax the first assumption tend to favor more adaptive substitutions on autosomes (23, 25, 26). The second assumption has received much less scrutiny, though previous models have considered systematic

differences in the overall mutation rate or efficacy of selection between the X and autosomes [e.g., due sex-biased mutation rates, potential consequences of dosage compensation or its absence, and factors affecting  $N_e$  on the X relative to the autosomes (24, 28, 29)]. Nevertheless, these considerations cannot easily account for empirical patterns of faster-X adaptive substitution unless beneficial mutations are often recessive with respect to fitness (26).

By explicitly modeling the distribution of fitness effects of new mutations using Fisher’s geometric model—and therefore allowing mutations to be overdominant—we find that the tempo of adaptive substitutions on the X is systematically elevated across a broad spectrum of dominance conditions. Predictions of traditional faster-X theory (24, 26) emerge in the special case where the phenotypic effect sizes of random mutations are small relative to the distance of the population to its phenotypic optimum. Yet these earlier predictions break down as mutation sizes increase relative to the distance of the population to its optimum. Our results suggest that we should be wary about interpreting elevated X-linked adaptive substitution rates as evidence that beneficial mutations are typically recessive. Instead, faster-X adaptive substitution rates can also occur when beneficial mutations are dominant to overdominant with respect to fitness (i.e.,  $h > 0.5$ ), which aligns with predictions of leading theories of dominance (14). While this reconciles the apparent contradiction between theories of dominance and typical interpretations of empirical faster-X adaptive substitution patterns, further investigation is required to assess whether beneficial mutations do indeed tend to be dominant (we return to this point further below).

One obvious question is whether we should expect mutation sizes to be small enough for traditional faster-X theory to apply or large enough for faster-X adaptive substitution rates to emerge across a broader range of dominance conditions. Here, it is important to recall the definition of mutation “size” in Fisher’s model ( $x = r\sqrt{n}/(2z)$ , as defined above), which depends on the absolute effect size of the mutation ( $r$ ) relative to the distance of the population to the optimum ( $z$ ). Mutations should often have large effects in Fisher’s scale if populations are reasonably well-adapted to their environments, as we expect them to be, even in cases where there is scope for further adaptation (67). The common observation from mutation accumulation studies that random mutations are much

more likely to reduce than to enhance fitness is consistent with mutation sizes being large, on average, in Fisher's scale (see ref. 68 for a critical review of mutation accumulation studies). For example, if we assume that 10% of new mutations are homozygous beneficial and mutation sizes are exponentially distributed, the corresponding mean size of new mutations is  $\bar{x} \approx 3.2$  (56), which falls comfortably in the range where mutations experience substantially more positive selection on the X. Moreover, while we do not know the distribution of scaled mutation sizes in any population, our assumption that the distribution of  $x$  is exponential should make our predictions conservative. Under the exponential, the probability density function for  $x$  is maximized at zero, causing a large fraction of beneficial mutations to have small effects, even in our "large-mutation limit" (naturally, all mutations have small effects in the "small-mutation limit"). Versions of Fisher's geometric model that assume a mutation size distribution with an intermediate mode (e.g., refs. 57, 66, 69) should reduce the fraction of mutations with small effects and enhance the tendency of X-linked genes to adapt more rapidly than autosomal genes.

Our analysis assumes that adaptation proceeds by fixation of positively selected alleles that arise by mutation and sweep through an initially monomorphic population (*SI Appendix, Appendix 1 and 2*), or a population initially segregating for a balanced polymorphism (*SI Appendix, Appendix 4 and 5*). This opens two avenues for future work. First, Orr and Betancourt (23) showed that adaptation from standing genetic variation is more permissive on the autosomes relative to the X, yet their analysis did not account for the higher incidence of positive selection among X-linked relative to autosomal variants, which we observe in Fisher's geometric model (e.g., Fig. 3*B*). A higher prevalence of positive selection on the X might, at least in some cases, result in a higher X-linked than autosomal probability of a selective sweep arising from standing genetic variation, though this intuition requires formal validation. Second, adaptation can be polygenic, with many segregating alleles in the genome simultaneously responding to selection of traits to their optimum. Though it is unclear how "typical" this form of adaptation is (70, 71), evidence from genome-wide association studies and sustained responses to artificial selection implies that polygenic adaptation affects many traits (72). Such a scenario appears to be beyond the scope of analytical treatment, though an intensive simulation study that tracks genome-wide patterns of substitution during adaptation to a fixed or moving optimum (e.g., ref. 73) would help in evaluating how polygenicity might influence faster-X predictions.

While our models focus on rates of positively selected substitution, empirical estimates of adaptive substitution based on MK tests (e.g., the studies summarized in Fig. 1*B*) are based on comparisons between within-species polymorphism and between-species substitutions (31, 58). In this framework, two main factors can enhance X-linked relative to autosomal signals of adaptive substitution. First and most obviously, faster-X signals should emerge when rates of positively selected substitutions are elevated on the X, owing to either recessivity of beneficial mutations (24, 26) or a higher prevalence of positively selected mutations on the X than the autosomes (e.g., as we have found here). Second, faster-X signals might at least partially reflect elevated ratios of nonsynonymous-to-synonymous polymorphism on autosomes relative to the X. MK tests for adaptive divergence are downwardly biased when nonneutral variants contribute to polymorphism (64, 74, 75), and we typically expect higher levels of deleterious and balanced polymorphism on autosomes than the X (34, 51, 52, 76). Bias caused by deleterious mutations can be minimized by excluding rare polymorphic variants from MK analyses (31, 74, 75, 77) and by using metrics that exclude nearly neutral

substitutions (e.g.,  $\omega_A$  rather than  $\alpha$ ; see ref. 31). However, bias caused by overdominant polymorphisms is not so easily controlled and could plausibly exacerbate MK-based signals of faster-X adaptive substitution.

Comparisons between X chromosomes and autosomes are interesting and informative for understanding a myriad of evolutionary processes (78–80). However, the model presented here suggests that X/autosome comparisons will only remain informative about the dominance of adaptive mutations when populations are consistently and strongly displaced from their optima, in which case (scaled) mutation sizes will be sufficiently small for classical faster-X predictions to apply. Strong displacements might arise in natural populations that continuously "chase" a rapidly moving optimum. They might also arise for genes that have recently arisen via duplication [and are therefore far away from their optimum (70)], or for genes that experience rapidly changing environments of selection [e.g., genes involved in immunity (81)]. X/autosome comparisons in "evolve-and-resequence" studies might also be informative if carried out across a gradient of environmental change scenarios, such as laboratory treatments with different degrees of environmental novelty or stress.

Additional methods, while perhaps imperfect, will undoubtedly help characterize the dominance of new beneficial mutations. One method is to experimentally measure the dominance of putatively adaptive variants that have evolved in predominantly haploid or self-fertilizing populations, where the fates of adaptive variants are not directly influenced by effects of dominance (for relevant examples, see refs. 17, 18, 82–84). There are some potential issues with this approach. For example, the dominance coefficients and homozygous selection coefficients of mutations could be correlated, in which case the preferential establishment of beneficial alleles with large homozygous beneficial effects will lead to differences between the dominance of new mutations and those contributing to adaptation. There is also some uncertainty about the alignment of mutant fitness effects when expressed in the haploid versus homozygous diploid state (85, 86), which can also confound interpretations of dominance through comparisons of haploid versus diploid individuals. Finally, direct estimates of dominance among mutations contributing to adaptation in outbred, diploid populations are likely to carry useful information about the distribution of dominance among new mutations. For example, estimates of the distribution of dominance for fixed mutations (e.g., as inferred for domestication QTL in ref. 17) can be used to infer the distribution of new mutations, assuming that adaptation proceeds from new mutations [as might be the case for species with relatively low  $N_e$ , where adaptation from standing genetic variation is less likely (87)]. At minimum, the distribution for fixed variants should provide an upper bound for the dominance of new beneficial mutations, and careful modeling of the data can define a lower bound, once differential rates of establishment for beneficial mutation that vary in dominance (i.e., Haldane's sieve) are accounted for.

## Materials and Methods

The structure of our analysis follows classical models of faster-X evolution (e.g., refs. 26, 28; Fig. 1*A*) in that we focus on species with XY sex determination with a degenerate Y chromosome, where hemizygotes are phenotypically equivalent to homozygotes (e.g., due to dosage compensation). As in previous models, the rate of positively selected substitutions is modeled as the product of the population-scaled mutation rate to positively selected alleles and their average fixation probability. Our analysis differs from prior faster-X theory in that we explicitly model the relative rates of mutation to, and the fitness effects of, positively selected alleles (as in refs. 14 and 50), fitness effects are endogenous to our model rather than

being exogenous inputs). We focus on species with XY sex chromosome systems, but our results also apply to species with Z and W chromosomes.

**Using Fisher's Geometric Model to Generate Fitness Effects of New Mutations.** Here, we outline the simplest version of our model, in which we assume a monomorphic population with ancestral alleles initially fixed at each locus in the genome. We later relax this assumption by considering populations that segregate for intermediate-frequency balanced polymorphisms (SI Appendix, Appendix 4 and 5 for details). The ancestral phenotype is defined by the vector  $\mathbf{A} = (A_1, A_2, \dots, A_n)$ , where  $A_i$  is the ancestral phenotype for the  $i$ th of  $n$  traits. The phenotypic optimum is defined by the vector  $\mathbf{O} = (O_1, O_2, \dots, O_n)$ , where  $O_i$  is the optimum for the  $i$ th trait. The distance between the ancestral phenotype and the optimum is  $z = \sqrt{\sum_{i=1}^n (O_i - A_i)^2}$ . Homozygous (or hemizygous) carriers of a given mutation express phenotype  $\mathbf{A}_{\text{hom}} = (A_1 + \delta_1, A_2 + \delta_2, \dots, A_n + \delta_n)$  where  $\delta_i$  is the phenotypic effect of the mutation in the  $i$ th trait;  $r = \sqrt{\sum_{i=1}^n \delta_i^2}$  is the total size of the phenotypic effect of a given mutation. Heterozygotes for the mutation express phenotype  $\mathbf{A}_{\text{het}} = (A_1 + v\delta_1, A_2 + v\delta_2, \dots, A_n + v\delta_n)$ , where  $v$  is the dominance of the mutation with respect to the phenotype ("phenotypic dominance", which we assume takes a fixed value within the range  $0 < v < 1$  and excludes completely recessive or dominant phenotypic effects; see ref. 14). The distance to the optimum for heterozygotes and homozygotes of a given mutation is  $z_{\text{het}} = \sqrt{\sum_{i=1}^n (O_i - A_i - v\delta_i)^2}$  and  $z_{\text{hom}} = \sqrt{\sum_{i=1}^n (O_i - A_i - \delta_i)^2}$ , respectively.

There is an important distinction between phenotypic dominance ( $v$ ) and dominance with respect to fitness (i.e.,  $h = s_{\text{het}}/s_{\text{hom}}$ , where  $s_{\text{het}}$  is the heterozygous and  $s_{\text{hom}}$  is the homozygous fitness effect of a given mutation), with the latter being the focus of prior faster-X models. Manna et al. (14) showed that for a population near its optimum, the fitness effects of random mutations—which are predominantly deleterious—tend to be partially recessive even in the absence of dominance at the phenotypic level (i.e.,  $h \sim 1/4$  for deleterious mutations when  $v = 1/2$ ). We retrieve the same result for populations converging to the optimum ( $z \rightarrow 0$ ), which causes all mutations to be deleterious, and those with mild fitness effects to exhibit dominance coefficients of  $h \approx v^2$  (SI Appendix, Appendix 3). For adaptive mutations—our focus here—the relation between  $v$  and  $h$  in Fisher's geometric model depends on the distribution of mutation sizes (SI Appendix, Figs. S1 and S2). Here, the two forms of dominance are roughly equivalent ( $h \approx v$ ) in the special case of mutations with infinitesimally small phenotypic effect sizes, and  $h > v$  otherwise (SI Appendix, Appendix 3). For tractability, we present analytical results in terms of  $v$  and numerical results in terms of both  $h$  and  $v$ . We also derive approximations for the relation between  $v$  and  $h$  in SI Appendix, Appendix 3 (SI Appendix, Fig. S1 and S2).

We assume that mutation magnitudes (values of  $r$ ) are exponentially distributed with a mean of  $\bar{r}$ . When scaled relative to the ancestral distance to the optimum, mutation magnitudes are  $x = r\sqrt{n}/(2z)$  (53, 54) and the distribution of  $x$  is exponential with mean  $\bar{x} = \bar{r}\sqrt{n}/(2z)$ . Mutation orientations are randomly distributed in  $n$ -dimensional phenotypic space (i.e., we assume isotropy). The orientation of a random mutation with magnitude  $r$  is defined by the vector of trait displacements:

$$\delta | r = \frac{1}{\sqrt{\sum_{j=1}^n y_j^2}} (ry_1, ry_2, \dots, ry_{n-1}, ry_n), \quad [10]$$

where  $y_1, y_2, \dots, y_n$  are independent standard normal random variables (55, 56).

Fitness is a Gaussian function of the distance to the optimum (50, 53, 54, 56, 57). Fitness of the ancestral homozygote is  $w = e^{-z^2/2}$ , and fitness of heterozygous and homozygous carriers of a given mutation is  $w_{\text{het}} = e^{-z_{\text{het}}^2/2}$  and  $w_{\text{hom}} = e^{-z_{\text{hom}}^2/2}$ . The corresponding heterozygous and homozygous selection coefficients are:

$$s_{\text{het}} = \frac{w_{\text{het}}}{w} - 1 = \exp\left(-\frac{1}{2}v^2r^2 + v \sum_{i=1}^n (O_i - A_i)\delta_i\right) - 1. \quad [11a]$$

$$s_{\text{hom}} = \frac{w_{\text{hom}}}{w} - 1 = \exp\left(-\frac{1}{2}r^2 + \sum_{i=1}^n (O_i - A_i)\delta_i\right) - 1. \quad [11b]$$

Previous work has shown that, with high dimensionality ( $n > \sim 10$ ) and weak selection, the distribution of heterozygous and homozygous selection coefficients for mutations with specified magnitude  $r$  is approximately bivariate normal with respective means of  $\bar{s}_{\text{het}} = -\frac{1}{2}(vr)^2$  and  $\bar{s}_{\text{hom}} = -\frac{1}{2}r^2$ , and variances of  $\sigma_{\text{het}}^2 = (vz)^2/n$  and  $\sigma_{\text{hom}}^2 = (rz)^2/n$ . Selection coefficients are perfectly correlated, such that  $s_{\text{het}} = \frac{1}{2}r^2v(1-v) + vs_{\text{hom}}$  (56). We use these approximations in our analytical results and validate them by simulation.

**Probabilities of Fixation for Positively Selected Mutations.** For autosomal loci, mutations are easily categorized by their modes of selection, which include positive selection ( $s_{\text{hom}} \geq s_{\text{het}} \gg 0$ ; blue in Fig. 2), purifying selection ( $s_{\text{het}} < 0$ , gray in Fig. 2), and balancing selection in cases of overdominance for fitness ( $s_{\text{hom}} < s_{\text{het}} > 0$ ; orange and red in Fig. 2). The conditions for positive selection are more permissive for the X than the autosomes. In addition to mutations in the range  $s_{\text{hom}} \geq s_{\text{het}} \gg 0$ , which experience positive selection on both the autosomes and the X, a subset of overdominant mutations also evolves under positive selection when X-linked (e.g., the orange mutations in Fig. 2, which are deterministically favored to fix on the X but not on the autosomes).

Conditions for positive selection on the X chromosome depend on the manner with which mutations are expressed in each sex. We first consider mutations with equal expression between the sexes (i.e., homozygous phenotypic effects in females are equal to hemizygous effects in males). An X-linked mutation experiences positive selection under the condition:

$$0 < s_{\text{het}} \leq \frac{s_{\text{hom}}(3 + 2s_{\text{hom}})}{2 + s_{\text{hom}}}, \quad [12]$$

(SI Appendix, Appendix 1), which under weak selection simplifies, approximately, to  $0 < s_{\text{het}} \leq \frac{3}{2}s_{\text{hom}}$ . Using normal approximations for the distributions of  $s_{\text{het}}$  and  $s_{\text{hom}}$ , which apply when the fitness effects of mutations are small (SI Appendix, Appendix 1 and ref. 56), the probability that a random mutation of magnitude  $r$  meets the condition for positive selection is:

$$\Pr(\text{pos. } | A, r) \approx \Pr\left(s_{\text{hom}} \geq \frac{1}{2}r^2v\right) = 1 - \Phi\left(\frac{r\sqrt{n}}{2z}(1+v)\right), \quad [13a]$$

for the autosomes, and:

$$\begin{aligned} \Pr(\text{pos. } | X, r) &\approx \Pr\left(s_{\text{hom}} \geq \frac{r^2v(1-v)}{3-2v}\right) \\ &= 1 - \Phi\left(\frac{r\sqrt{n}}{2z}\left(1 + \frac{2v(1-v)}{3-2v}\right)\right), \end{aligned} \quad [13b]$$

for the X, where  $\Phi(\cdot)$  is the cumulative density function for the standard normal distribution (SI Appendix, Appendix 1).

The fixation probability for a new, positively selected mutation is approximately  $2s_{\text{het}}$  under autosomal linkage and  $2(2s_{\text{het}} + s_{\text{hom}})/3$  under X-linkage (23, 24, 26). Incorporating distributions of fitness effects, the probability that a mutation with magnitude  $r$  both meets the condition for positive selection and becomes fixed is:

$$\Pr(\text{fix} | A, r) \approx \int_{\frac{1}{2}r^2v}^{\infty} 2s_{\text{het}} f(s_{\text{hom}}) ds_{\text{hom}}, \quad [14]$$

under autosomal linkage, and:

$$\Pr(\text{fix} | X, r) \approx \int_{\frac{r^2v(1-v)}{3-2v}}^{\infty} \frac{2}{3}(2s_{\text{het}} + s_{\text{hom}}) f(s_{\text{hom}}) ds_{\text{hom}}, \quad [15]$$

under X-linkage, where  $f(s_{hom})$  is the probability density function for  $s_{hom}$  and  $s_{het}$  is a function of  $s_{hom}$  (SI Appendix, Appendix 2).

For mutations with male-limited expression (which are neutral in females), the condition for positive selection remains the same for autosomal genes (i.e.,  $0 < s_{het} \leq s_{hom}$ ), while the condition for X-linked mutations becomes  $s_{hom} \gg 0$ . Fixation probabilities for positively selected variants are approximately  $s_{het}$  for autosomes and  $2s_{hom}/3$  for the X (as in ref. 26). The probability that an X-linked mutation with magnitude  $r$  both meets the conditions for positive selection and becomes fixed is:

$$\Pr(\text{fix}|X, r) \approx \int_0^{\infty} \frac{2}{3} s_{hom} f(s_{hom}) ds_{hom}. \quad [16]$$

The corresponding probability for the autosomes is obtained by dividing Eq. 14 by two.

**Simulations.** Analytical approximations were tested against exact computer simulations, in which the selection coefficients of random mutations were generated using Eqs. 10–11. Mutations that met exact criteria for positive selection (e.g., Eq. 12) were introduced as a single initial copy in a Wright–Fisher population with effective size  $N$  and an equal sex ratio of breeding adults (corresponding to  $2N$  autosomes and  $1.5NX$  chromosomes in breeding adults of each generation). We simulated genetic drift by carrying out multinomial sampling of each genotype,

with sampling probabilities based on deterministic predictions of genotype frequencies in breeding adults (see pp. 229–230 in ref. 88).

In these simulations, X chromosomes and autosomes compete to fix the next positively selected mutation. Each mutation was introduced on the X or autosome with respective probabilities 3/7 and 4/7 (reflecting three X-linked copies for every four autosomes) and was fixed or lost prior to the introduction of the next mutation. We tallied the total number of mutations fixed and the proportion fixed on each chromosome. To examine how mutations under balancing selection might also contribute to empirical signals of adaptive substitution, we ran additional simulations that tracked fixation events for mutations whose homozygous fitness effects were positive ( $s_{hom} > 0$ , corresponding to deterministic equilibrium frequencies greater than 0.5), which includes alleles under positive selection and balancing selection. For these simulations, a mutation was recorded as contributing to the adaptive substitutions if it fixed within  $4N$  generations on an autosome or  $3N$  generations on the X, which represent the standard neutral benchmarks for each chromosome (63).

**Data, Materials, and Software Availability.** All study data are included in the article and/or supporting information.

**ACKNOWLEDGMENTS.** This work was supported by funds from the Australian Research Council and The School of Biological Sciences at Monash University. F.R. was funded by a H2020 Marie Skłodowska–Curie COFUND Action (No. 101034413). We thank three anonymous reviewers for suggestions that substantially improved the paper and breadth of the analysis.

1. S. Billiard, V. Castric, V. Laurens, The integrative biology of genetic dominance. *Biol. Rev.* **96**, 2925–2942 (2021).
2. S. P. Otto, The advantages of segregation and the evolution of sex. *Genetics* **164**, 1099–1118 (2003).
3. M. Hartfield, P. D. Keightley, Current hypotheses for the evolution of sex and recombination. *Integrative Zool.* **7**, 192–209 (2012).
4. B. Charlesworth, Causes of natural variation in fitness: Evidence from studies of *Drosophila* populations. *Proc. Natl. Acad. Sci. U.S.A.* **112**, 1662–1669 (2015).
5. S. F. Bailey, T. Bataillon, Can the experimental evolution programme help us elucidate the genetic basis of adaptation in nature? *Mol. Ecol.* **25**, 203–18 (2016).
6. J. B. S. Haldane, The effect of variation on fitness. *Am. Nat.* **735**, 337–349 (1937).
7. D. Charlesworth, B. Charlesworth, Inbreeding depression and its evolutionary consequences. *Annu. Rev. Ecol. Syst.* **18**, 237–268 (1987).
8. B. Charlesworth, Evolutionary rates in partially self-fertilizing species. *Am. Nat.* **140**, 126–148 (1992).
9. H. A. Orr, The population genetics of beneficial mutations. *Phil. Trans. Roy. Soc. B.* **365**, 1195–201 (2010).
10. T. Connallon, M. D. Hall, Genetic constraints on adaptation: A theoretical primer for the genomics era. *Ann. NY Acad. Sci.* **1422**, 65–87 (2018).
11. H. Uecker, Evolutionary rescue in randomly mating, selfing, and clonal populations. *Evolution* **71**, 845–858 (2017).
12. M. J. Simmons, J. F. Crow, Mutations affecting fitness in *Drosophila* populations. *Annu. Rev. Genet.* **11**, 49–78 (1977).
13. D. L. Halligan, P. D., Keightley Spontaneous mutation accumulation studies in evolutionary genetics. *Annu. Rev. Ecol. Syst.* **40**, 151–172 (2009).
14. F. Manna, G. Martin, T. Lenormand, Fitness landscapes: An alternative theory for the dominance of mutation. *Genetics* **189**, 923–937 (2011).
15. A. F. Agrawal, M. C. Whitlock, Inferences about the distribution of dominance drawn from yeast gene knockout data. *Genetics* **187**, 553–566 (2011).
16. T. Bataillon, S. F. Bailey, Effects of new mutations on fitness: Insights from models and data. *Ann. NY Acad. Sci.* **1320**, 76–92 (2014).
17. J. Ronfort, S. Glemin, Mating system, Haldane's sieve, and the domestication process. *Evolution* **67**, 1518–1526 (2013).
18. A. C. Gerstein, A. Kuzmin, S. P. Otto, Loss-of-heterozygosity facilitates passage through Haldane's sieve for *Saccharomyces cerevisiae* undergoing adaptation. *Nat. Commun.* **5**, 3819 (2014).
19. A. E. van't Hof, et al., The industrial melanism mutation in British peppered moths is a transposable element. *Nature* **534**, 102–105 (2016).
20. K. Grieshop, E. K. H. Ho, K. R. Kasimatis, Dominance reversals: The resolution of genetic conflict and maintenance of genetic variation. *Proc. Roy. Soc. B* **291**, 20232816 (2024).
21. D. Sellis, D. J. Kvitik, B. Dunn, G. Sherlock, D. A. Petrov, Heterozygote advantage is a common outcome of adaptation in *Saccharomyces cerevisiae*. *Genetics* **203**, 1401–1413 (2016).
22. D. Aggeli, et al., Overdominant and partially dominant mutations drive clonal adaptation in diploid *Saccharomyces cerevisiae*. *Genetics* **221**, iyac061 (2022).
23. H. A. Orr, A. J. Betancourt, Haldane's sieve and adaptation from the standing genetic variation. *Genetics* **157**, 875–884 (2001).
24. B. Charlesworth, J. A. Coyne, N. H. Barton, The relative rates of evolution of sex chromosomes and autosomes. *Am. Nat.* **130**, 113–146 (1987).
25. T. Connallon, N. D. Singh, A. G. Clark, Impact of genetic architecture on the relative rates of X versus autosomal adaptive substitution. *Mol. Biol. Evol.* **29**, 1933–1942 (2012).
26. B. Charlesworth, J. L. Campos, B. C. Jackson, Faster-X evolution: Theory and evidence from *Drosophila*. *Mol. Ecol.* **27**, 3753–3771 (2018).
27. A. Mrnjavac, K. A. Khudiakova, N. H. Barton, B. Vicoso, Slower-X: Reduced efficiency of selection in the early stages of X chromosome evolution. *Evol. Letters* **7**, 4–12 (2023).
28. M. Kirkpatrick, D. W. Hall, Male-biased mutation, sex linkage, and the rate of adaptive evolution. *Evolution* **58**, 437–440 (2004).
29. B. Vicoso, B. Charlesworth, Effective population size and the faster-X effect: An extended model. *Evolution* **63**, 2413–2426 (2009).
30. R. L. Unckless, H. A. Orr, The population genetics of evolutionary rescue in diploids: X chromosomal versus autosomal rescue. *Am. Nat.* **195**, 561–568 (2020).
31. N. Galtier, Adaptive protein evolution in animals and the effective population size hypothesis. *PLoS Genet.* **12**, e1005774 (2016).
32. C. Hvilsoe, et al., Extensive X-linked adaptive evolution in central chimpanzees. *Proc. Natl. Acad. Sci. U.S.A.* **109**, 2054–2059 (2012).
33. A. Kousathanas, D. L. Halligan, P. D. Keightley, Faster-X adaptive protein evolution in house mice. *Genetics* **196**, 1131–1143 (2014).
34. K. R. Veeramah, R. N. Gutenkunst, A. E. Woerner, J. C. Watkins, M. F. Hammer, Evidence for Increased Levels of Positive and Negative Selection on the X Chromosome versus Autosomes in Humans. *Mol. Biol. Evol.* **31**, 2267–2282 (2014).
35. J. L. Campos, D. L. Halligan, P. R. Haddrill, B. Charlesworth, The relation between recombination rate and patterns of molecular evolution and variation in *Drosophila melanogaster*. *Mol. Biol. Evol.* **31**, 1010–1028 (2014).
36. D. Garrigan, S. B. Kingan, A. J. Geneva, J. P. Vedanayagam, D. C. Presgraves, Genome diversity and divergence in *Drosophila mauritiana*: Multiple signatures of faster X evolution. *Genome Biol. Evol.* **6**, 2444–2458 (2014).
37. A. Pinharanda, et al., Sexually dimorphic gene expression and transcriptome evolution provide mixed evidence for a fast-Z effect in *Heliconius*. *J. Evol. Biol.* **32**, 194–204 (2019).
38. M. Carneiro, et al., Evidence for widespread positive and purifying selection across the European rabbit (*Oryctolagus cuniculus*) genome. *Mol. Biol. Evol.* **29**, 1837–1849 (2012).
39. V. Avila, et al., Faster-X effects in two *Drosophila* lineages. *Genome Biol. Evol.* **6**, 2968–2982 (2014).
40. M. Rousselle, N. Faivre, M. Ballenghien, N. Galtier, B. Nabholz, Hemizyosity enhances purifying selection: Lack of fast-Z evolution in two Satyrine butterflies. *Genome Biol. Evol.* **8**, 3108–3119 (2016).
41. K. Hayes, H. J. Barton, K. Zeng, A study of faster-Z evolution in the great tit (*Parus major*). *Genome Biol. Evol.* **12**, 210–222 (2020).
42. M. A. Chase, M. Vilcot, C. F. Mugal, Evidence that genetic drift not adaptation drives fast-Z and large-Z effects in *Ficedula* flycatchers. *Mol. Ecol.* <https://doi.org/10.1111/mec.17262> (2024).
43. A. J. Mongue, M. E. Hansen, J. R. Walters, Support for faster and more adaptive Z chromosome evolution in two divergent lepidopteran lineages. *Evolution* **76**, 332–345 (2022).
44. M. Harris, N. R. Garud, Enrichment of hard sweeps on the X chromosome in *Drosophila melanogaster*. *Mol. Biol. Evol.* **40**, msac268 (2023).
45. M. Harris, B. Kim, N. Garud, Enrichment of hard sweeps on the X chromosome compared to autosomes in six *Drosophila* species. *Genetics* **226**, iyae019 (2024).
46. S. Wright, Molecular and evolutionary theories of dominance. *Am. Nat.* **68**, 24–53 (1934).
47. J. H. Gillespie, A general model to account for enzyme variation in natural populations. IV. The quantitative genetics of viability mutants, Lecture Notes in Biomathematics, in *Measuring Selection in Natural Populations*, F. B. Christiansen, T. M. Fenchel, Eds. (Springer, 1977), pp. 301–314.
48. B. Charlesworth, Evidence against Fisher's theory of dominance. *Nature* **278**, 848–849 (1979).
49. P. Muralidhar, C. Veller, Dominance shifts increase the likelihood of soft selective sweeps. *Evolution* **76**, 966–984 (2022).
50. D. Sellis, B. J. Callahan, D. A. Petrov, P. W. Messer, Heterozygote advantage as a natural consequence of adaptation in diploids. *Proc. Natl. Acad. Sci. U.S.A.* **108**, 20666–20671 (2011).
51. P. Madigan, Genetic variation at sex-linked loci: Quantification of regular selection models. *Hereditas* **91**, 129–133 (1979).

52. P. J. Avery, The population genetics of haplo-diploids and X-linked genes. *Genet. Res. Camb.* **44**, 321–341 (1984).
53. R. A. Fisher, *The Genetical Theory of Natural Selection* (Clarendon Press, Oxford, 1930).
54. H. A. Orr, The population genetics of adaptation: The distribution of factors fixed during adaptive evolution. *Evolution* **52**, 935–949 (1998).
55. T. Connallon, A. G. Clark, Evolutionary inevitability of sexual antagonism. *Proc. Roy. Soc. B.* **281**, 20132123 (2014).
56. Y. McDonough, T. Connallon, Effects of population size change on the genetics of adaptation following an abrupt change in environment. *Evolution* **77**, 1852–1863 (2023).
57. O. Tenaillon, The utility of Fisher's geometric model in evolutionary genetics. *Annu. Rev. Ecol. Evol. Syst.* **45**, 179–201 (2014).
58. A. Eyre-Walker, The genomic rate of adaptive evolution. *Trends Ecol. Evol.* **21**, 569–575 (2006).
59. J. K. Pritchard, J. K. Pickrell, G. Coop, The genetics of human adaptation: Hard sweeps, soft sweeps, and polygenic adaptation. *Curr. Biol.* **20**, R208–R215 (2010).
60. A. J. Betancourt, Y. Kim, H. A. Orr, A pseudohitchhiking model of X vs. autosomal diversity. *Genetics* **168**, 2261–2269 (2004).
61. A. Robertson, Selection for heterozygotes in small populations. *Genetics* **47**, 1291–1300 (1962).
62. M. Nei, A. K. Roychoudhury, Probability of fixation and mean fixation time of an overdominant mutation. *Genetics* **74**, 371–80 (1973).
63. K. Kimura, T. Ohta, The average number of generations until fixation of a mutant gene in a finite population. *Genetics* **61**, 763–771 (1969).
64. S. Williamson, A. Fledel-Alon, C. D. Bustamante, Population genetics of polymorphism and divergence for diploid selection models with arbitrary dominance. *Genetics* **168**, 463–475 (2004).
65. D. Waxman, J. J. Welch, Fisher's microscope and Haldane's ellipse. *Am. Nat.* **166**, 447–457 (2005).
66. G. Martin, T. Lenormand, A general multivariate extension of Fisher's geometrical model and the distribution of mutation fitness effects across species. *Evolution* **60**, 893–907 (2006).
67. H. A. Orr, The genetic theory of adaptation: A brief history. *Nat. Rev. Genet.* **6**, 119–127 (2005).
68. K. Bao, R. H. Melde, S. P. Sharp, Are mutations usually deleterious? A perspective on the fitness effects of mutation accumulation. *Evol. Ecol.* **36**, 753–766 (2022).
69. Z. Wang, B. Y. Liao, J. Zhang, Genomic patterns of pleiotropy and the evolution of complexity. *Proc. Natl. Acad. Sci. U.S.A.* **107**, 18034–18039 (2010).
70. A. F. Moutinho, A. Eyre-Walker, J. Y. Dutheil, Strong evidence for the adaptive walk model of gene evolution in *Drosophila* and *Arabidopsis*. *PLoS Biol.* **20**, e3001775 (2022).
71. K. Bombliès, C. L. Peichel, Genetics of adaptation. *Proc. Natl. Acad. Sci. U.S.A.* **119**, e2122152119 (2022).
72. G. Sella, N. H. Barton, Thinking about the evolution of complex traits in the era of genome-wide association studies. *Ann. Rev. Genomics Hum. Genet.* **20**, 461–493 (2019).
73. P. Muralidhar, G. Coop, Polygenic response of sex chromosomes to sexual antagonism. *Evolution* **78**, 539–554 (2024).
74. J. C. Fay, G. J. Wyckoff, C. I. Wu, Testing the neutral theory of molecular evolution with genomic data from *Drosophila*. *Nature* **415**, 1024–1026 (2002).
75. J. Charlesworth, A. Eyre-Walker, The McDonald-Kreitman test and slightly deleterious mutations. *Mol. Biol. Evol.* **25**, 1007–1015 (2008).
76. F. Ruzicka, T. Connallon, M. Reuter, Sex differences in deleterious mutational effects in *Drosophila melanogaster*: Combining quantitative and population genetic insights. *Genetics* **219**, iyab143 (2021).
77. P. W. Messer, D. A. Petrov, Frequent adaptation and the McDonald-Kreitman test. *Proc. Natl. Acad. Sci. U.S.A.* **110**, 8615–8620 (2013).
78. B. Vicoso, B. Charlesworth, Evolution on the X chromosome: Unusual patterns and processes. *Nat. Rev. Genet.* **7**, 645–653 (2006).
79. M. A. Wilson Sayres, Genetic diversity on the sex chromosomes. *Genome Biol. Evol.* **10**, 1064–10978 (2018).
80. F. Ruzicka, T. Connallon, Is the X chromosome a hot spot for sexually antagonistic polymorphisms? Biases in current empirical tests of classical theory. *Proc. Biol. Sci.* **287**, 20201869 (2020).
81. V. Soni, A. Eyre-Walker, Factors that affect the rates of adaptive and nonadaptive evolution at the gene level in humans and chimpanzees. *Genome Biol. Evol.* **14**, evac028 (2022).
82. J. B. Anderson, C. Sirjusingh, N. Ricker, Haploidy, diploidy and evolution of antifungal drug resistance in *Saccharomyces cerevisiae*. *Genetics* **168**, 1915–1923 (2004).
83. D. A. Marad, S. W. Buskirk, G. I. Lang, Altered access to beneficial mutations slows adaptation and biases fixed mutations in diploids. *Nature Ecol. Evol.* **2**, 882–889 (2018).
84. J. Y. Leu, S. L. Chang, J. C. Chao, L. C. Woods, M. J. McDonald, Sex alters molecular evolution in diploid experimental populations of *S. cerevisiae*. *Nat. Ecol. Evol.* **4**, 453–460 (2020).
85. A. C. Gerstein, Mutational effects depend on ploidy level: All else is not equal. *Biol. Lett.* **9**, 20120614 (2013).
86. N. P. Sharp, L. Sandell, C. G. James, S. P. Otto, The genome-wide rate and spectrum of spontaneous mutations differ between haploid and diploid yeast. *Proc. Natl. Acad. Sci. U.S.A.* **115**, E5046–E5055 (2018).
87. M. Rousselle *et al.*, Is adaptation limited by mutation? A timescale-dependent effect of genetic diversity on the adaptive substitution rate in animals. *PLoS Genet.* **16**, e1008668 (2020).
88. B. Charlesworth, D. Charlesworth, *Elements of Evolutionary Genetics* (Roberts and Company Publishers, 2010).